Journal of Sensor Science and Technology
Vol. 33, No. 6 (2024) pp. 458-473
http://dx.doi.org/10.46670/JSST.2024.33.6.458
pISSN 1225-5475/eISSN 2093-7563

Functional Materials Based Surface Acoustic Wave Sensors: A Mini Review

Na Yoon Kim[1,*], Min Gyu Seo[1,*], See Jin Ryoo[1,*], Kyeong Jun Park[1,*], Hohyun Keum[2,+], and Hoe Joon Kim[1,+]

Abstract

Surface acoustic wave (SAW) sensors are widely recognized for their high sensitivity and reliability, which make them suitable for diverse applications. However, they continue to face limitations in repeatability, detection limits, and effective use in extreme environments as well as in biosensing and industrial settings. A critical factor in enhancing the performance of SAW sensors lies not only in the selection of advanced sensing materials but also in the precise methods of material integration. Recent advancements have combined nanostructured materials, which improve the surface characteristics, with analyte-specific substances that strengthen interactions, resulting in heightened sensitivity and accuracy. This review categorizes recent SAW sensor studies based on their applications and materials and provides an extensive overview for researchers. Additionally, it highlights how integration techniques affect the uniformity, thickness, and stability of the sensing films, all of which are essential for high-performance sensors. This study aimed to serve as a valuable resource for the development of SAW sensors with high reliability and longevity under challenging conditions.

Keywords: Surface acoustic wave, Chemical sensor, Biosensor, Gas sensor, VOC sensors, Functional material, Piezoelectric, Resonator

1. INTRODUCTION

There is growing interest in the development of sensitive sensors for real-time monitoring in various fields, such as process control of industrial equipment, monitoring of environmental hazards, and disease diagnosis. Sensors with different conversion mechanisms have been developed, including capacitive micromachined, optical, photonic crystal, acoustic, and chemiresistive sensors. Among them, acoustic sensors, namely surface acoustic wave (SAW) devices, have a lot of potential as sensors [1-3].

SAW sensors can detect a variety of factors, such as temperature, pressure, conductivity, and mass, as well as changes in the properties of a wave, such as frequency and amplitude. Because the waves generated by the surface on which the sensing material is incorporated change their properties through interactions with the analyte, they can be selectively and sensitively detected [4]. The SAW sensor can be used in sensing applications using an antenna that stimulates the SAW and can operate automatically without a battery, even under extremely harsh environmental conditions [5].

In addition, miniaturized SAW Sensors have an overwhelming advantage in terms of mobility if they process signals through wireless communication. Owing to their ease of fabrication and low cost, SAW devices have many applications, such as vapor, humidity, temperature, mass sensors, and biosensors [6-8]. However, they lack the ability to be actively used in industrial, biological, and extreme environments.

The sensitivity to a particular molecule is strongly influenced by the sensing material incorporated into the SAW sensor and the integration method, which is why new functionalized materials integrated with SAW sensors are constantly being researched.

This study provides comprehensive information on recent SAW sensors using functionalized sensing materials, including their sensing mechanism and integration techniques. Section 2 discusses the sensing mechanisms of SAW sensors categorized by design type. Section 3 introduces the recent developments in SAW sensor, categorizing six representative sensing materials, including functionalized nanocomposites. Section 4 elucidates the integration of sensing materials into SAW sensors, which is divided into six methods. Finally, in Section 5, we categorize the applications of SAW sensors that utilize functional sensing materials with examples.

[1]Department of Robotics and Mechatronics Engineering, Daegu Gyeongbuk Institute of Science and Technology (DGIST) Daegu 42988, Korea
[2]Digital Health Care R&D Department, Korea Institute of Industrial Technology (KITECH) Cheonan 31056, Korea
*These authors are contrubuted equally to this work.
[+]Corresponding author: joonkim@dgist.ac.kr, hkeum@kitech.re.kr
(Received : Oct. 29, 2024, Revised : Nov. 7, 2024, Accepted : Nov. 13, 2024)

Through the various SAW sensor research compiled in this paper, we hope that readers will have an opportunity to understand recent developments in SAW sensors and their new applications.

2. SAW SENSING MECHANISM

The SAW devices consist of two comb-shaped interdigital transducer (IDT) patterns fabricated on a piezoelectric material [9]. The materials used for IDT electrodes are mainly aluminum, platinum, copper, gold, and conducting ceramics. IDT electrode sets are periodic strips with uniform length, width, and spacing when used in sensing applications [10].

Fig. 1 (a) shows a two-port SAW resonator on a quartz substrate. Lc is the cavity length, and w is the acoustic aperture, which refers to the IDT finger overlap length [11,12].

Following the dynamic change in the electric input signal due to electromechanical coupling, mechanical energy is generated as an acoustic wave of the piezoelectric substrate [13]. The IDT serves as both the input and output electrodes, with one pole of the IDT electrically biased and the second pole grounded [14]. When

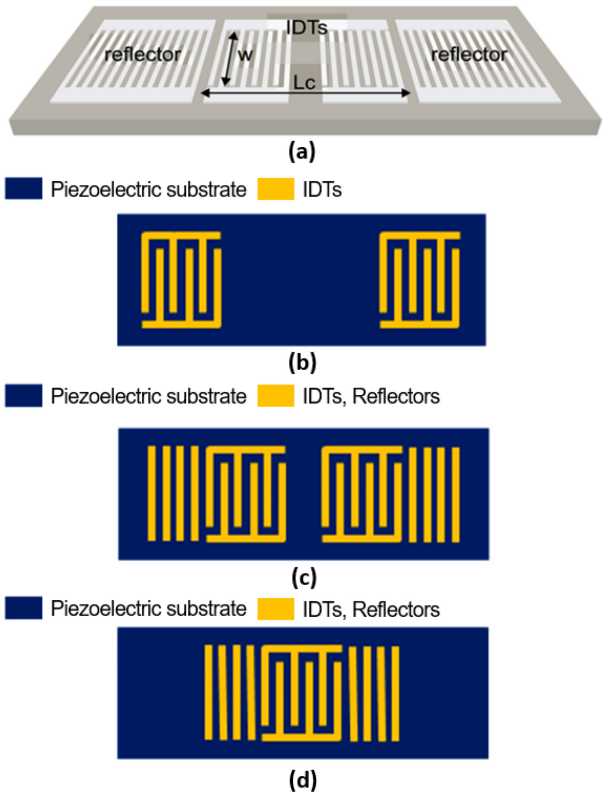

Fig. 1. SAW Device Structures: (a) Diagram of the 2-port SAW resonator. Reprinted with permission from Ref. [12]. Copyright (2024) MDPI. (b-d) Delay line configuration, two-port resonator, and one-port resonator. Reprinted with permission from Ref. [2]. Copyright (2024) MDPI. IDT: interdigital transducer.

an electrical sinusoidal wave with a period equivalent to the IDT pitch is applied, the piezoelectric material is periodically compressed owing to the alternating polarity of the electrodes. This results in oscillations under the IDT, producing the acoustic wave perpendicular to the IDT direction [15]. This wave confines and propagates along the surface of the piezoelectric material below the IDT [16]. This acoustic wave is converted back into electrical signal at the output end of IDT. Because the SAW energy propagates mainly through the surface area, slight changes in the surface conditions alter the signals received at the output IDT, which underlies the high sensitivity of SAW sensors.

Several physical parameters can influence SAW. Wave speed is an important parameter for SAW. The speed of the wave varies depending on the type of piezoelectric substrate, and the wave velocity can reduce the travel time between the IDTs. The wavelength of the SAW is also an important parameter. It is stimulated only when the applied signal wavelength matches the intrinsic wavelength of the SAW corresponding to the pitch of the IDT [17]. The following equation gives the relationship between the wave velocity, wavelength, and frequency:

$$f_0 = \frac{v}{\lambda}$$

where f_0 is the SAW resonance frequency, λ is the SAW wavelength vis the wave speed of the piezoelectric substrate. Typically, smaller IDT widths result in shorter wavelengths, which can increase a sensor's sensitivity by increasing its resonant frequency [18]. In certain applications, changing the width/spacing ratio of an IDT can produce higher harmonics [19].

Three structures can be used to design a SAW device: a delay line (DL), a two-port resonator (TPR), and a one-port resonator (OPR). Fig. 1 (b) shows the DL structure, which is usually an array of two sets of IDT that input and output electrical signals to and from a piezoelectric substrate [20]. The two IDT sets are separated by a distance that determines the delay path between the transmission and reception of the SAW. Once an electrical sinusoidal-wave signal is applied to the IDT at the input terminal that generates the surface wave, the wave is sent to the output IDT, which collects and analyzes the received signal. The area between the IDTs was coated with a sensing layer to allow interaction with the analyte. This area creates a time delay between the input and output signals depending on the wave path length and SAW speed [21].

Fig. 1 (c) shows a TPR consisting of an input IDT, an output IDT, and reflectors. The input terminal converts the electrical signal into a mechanical signal and transmits it, whereas the

output terminal converts the mechanical wave back into an electrical signal that it receives [22]. The electrodes deposited outside the IDT generate a resonant acoustic cavity with acoustic reflection electrode lattices [23]. They trap surface waves to form a resonant cavity with an enhanced SAW effect [24].

The third type of SAW structure is the OPR (Fig. 1 (d)). It comprises a set of IDT reflectors. Changes in the surface of the SAW resonator can alter its properties, rendering it a sensitive detector. The TPR is based on the insertion loss and high Q-factor of devices with a more stable circuit oscillation frequency, lower phase noise, and higher phase slope than DL and OPR [25].

Most SAW sensors sense by changing the resonant frequency, owing to the adsorption concentration of the analyte on the sensing material. This sensing mechanism is characterized by a frequency shift caused by mass loading, viscoelastic loading, and acoustoelectric loading. The dominant effect depends on the sensing material and device characteristics. The frequency change equation can be expressed as follows [26]:

$$\Delta f = -c_m f_o^2 \Delta\rho_s + c_e f_0^2 \Delta[hG'] - \frac{K_t^2}{2}\Delta\left[\frac{\sigma_s^2}{\sigma_s^2 + v_o^2 C_o^2}\right]$$

where h and ρ are the thickness and density of thin nonconducting layers, respectively. Δf is frequency shift, c_m denotes mass sensitivity coefficient, c_e denotes elasticity sensitivity coefficient, ρ_s is density of the adsorbent phase, G' denotes real part of the shear modulus, K_t^2 is the electromechanical coupling factor, v_o is unperturbed SAW velocity, and σ_s is sheet conductivity of the sensing film, C_0 is the capacitance per unit length of SAW substrate given by $C_0 = \varepsilon_s + \varepsilon_0$, where ε_s is the permittivity of substrate and ε_0 is the permittivity of free space.

In general, the first term of the equation, that is, the mass loading effect, is dominant, and the resonant frequency decreases with increasing concentration [27]. However, for certain sensing films, the second term of the equation, viscoelastic loading, becomes dominant due to hardening by analyte adsorption, which increases the resonant frequency with increasing concentration [28,29]. SAW sensors can also be found where the third term of the equation, the acoustoelectric loading, is dominant [30].

3. SENSING MATERIALS

The performance of SAW sensors is measured in terms of sensitivity, selectivity, response and recovery time, hysteresis, and lifetime. The most important factor determining these measurements is the sensing material. However, the sensor's performance also depends on the coating location, coating method, thickness, and uniformity of the sensing material. In the next section, we discuss the integration of the sensing materials in SAW devices.

In addition, the sensitivity of the SAW sensor can be increased by increasing its resonant frequency; however, because of noise, signal loss, and process limitations, improving the sensitivity of the SAW sensor via sensing material is a convenient approach. Many recent studies have improved sensing performance by functionalizing sensing materials with nanostructures that interact well with analytes. We introduce SAW sensors using functionalized nanocomposites and commonly used sensing materials in the following categories: metal oxide semiconductors (MOS), metal organic frameworks (MOF), carbon nanotubes (CNTs), graphene, noble metal nanoparticles, and polymers.

3.1 Metal Oxide Semiconductors

MOS has been widely used in chemical sensors, but they typically suffer from the disadvantage that they require operation under high-temperature conditions to achieve high sensing performance, such as selectivity and sensitivity. To improve the performance at low temperatures, research utilizing nanostructures, noble metal doping, and other techniques continues [31-33].

Zhou et al. [32] developed a SnO_2 SAW sensor that could measure NO_2 gas at room temperature by engineering the facets. A solvothermal method was utilized to fabricate SnO_2, and the growth time was adjusted to change the facets to achieve high adsorption capacities for NO_2. In this study, the facet-adjusted SnO_2 SAW sensor showed selectivity for NO_2 with a linear sensitivity of 17 kHz/10 ppm.

As a MOS, ZnO has the limitation that it needs to be operated at high temperatures to increase the sensing performance; however, this can be improved by doping ZnO with metal elements or organizing the nanostructure. Shu et al. [33] fabricated a SAW sensor to detect O_2 using ZnxFeyO films doped with Fe on ZnO as a sensing material. Fig. 2 (a) shows the scanning electron microscopy (SEM) image of a sample with a high Fe concentration [32]. The Fe doping of ZnO confirmed the performance improvement by doping, and the nanostructure configuration and the uniformity of the sensing film were improved by utilizing an oblique magnetron co-sputtering method for the synthesis of the SAW sensor and ZnxFeyO films. The frequency shift as a function of the amount of Fe doping indicated that the O_2 detection performance increased with increasing Fe doping.

ZnO, which is used in a variety of applications, can be utilized not only as a gas sensor but also as a UV sensor [34]. Walter

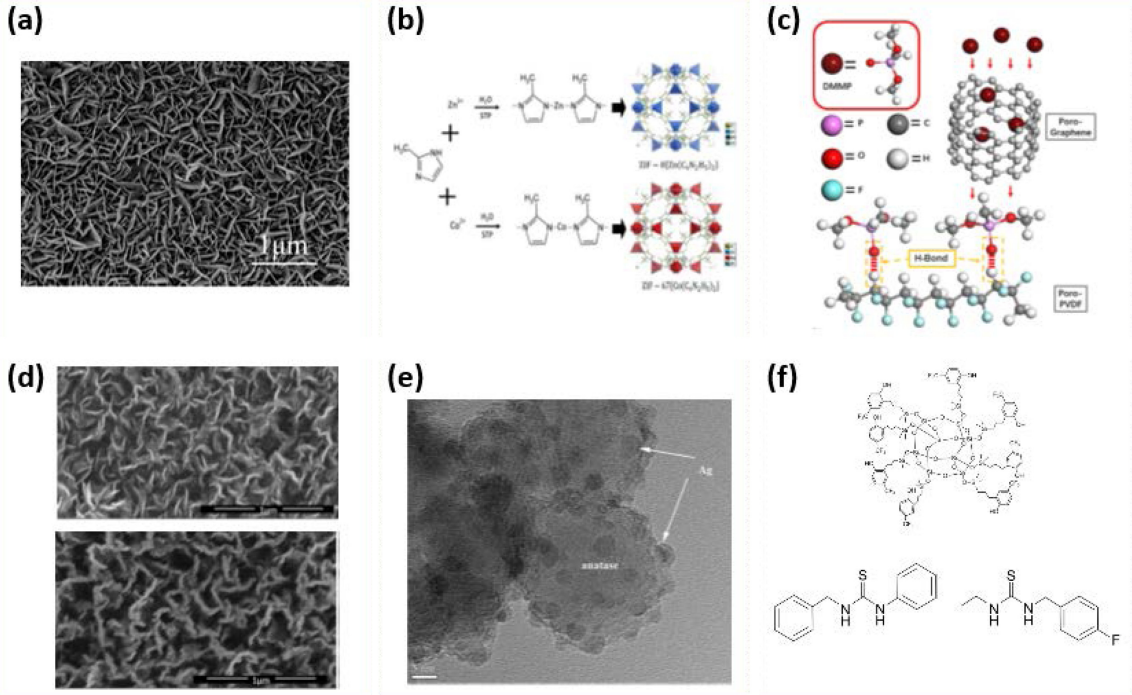

Fig. 2. Sensing materials: (a) SEM image of the ZnO sample with high Fe concentration. Reprinted with permission from Ref. [32]. Copyright (2019) MDPI. (b) Representative synthesis and crystal structures of ZIF-8 and ZIF-67 used as the sensitive layers of gas sensors. Reprinted with permission from Ref. [39]. Copyright (2018) MDPI. (c) Gas adsorption and hydrogen bond formation diagram of porous graphene/PVDF film. Reprinted with permission from Ref. [44]. Copyright (2021) MDPI. (d) SEM images of SAW@CNW sensor and SAW@CNW_Treat. Reprinted with permission from Ref. [46]. Copyright (2023) MDPI. (e) TEM image of the TWV-7-0@Ag. Reprinted with permission from Ref. [49]. Copyright (2024) MDPI. (f) Chemical structure of the sensing materials: POSS, TU-1 and TU-2. Reprinted with permission from Ref. [51]. Copyright (2020) MDPI.

Water and Ren-Yang Jhao [35] developed a SAW-based UV photodetector synthesized with ZnO nanorods by exploiting ZnO's ability to change its conductivity under UV light. As the ZnO nanorods formed by the hydrothermal method have much larger length-to-diameter and surface-to-volume ratios, they increase the area for UV absorption and charge concentration.

3.2 Metal Organic Frameworks

MOFs are porous skeletal structures composed of metals and organic materials. MOFs have many pores that enable them to adsorb certain molecules. They are characterized by tunability and structural diversity, where the pore size of the structure can be adjusted by changing the metal or organic. This tuning enabled the development of sensing materials with different chemical and physical properties. The sensing principle of MOFs is mainly based on the mass loading effect by the adsorption of molecules smaller than the pores and adsorption by chemical interactions such as hydrogen bonding [36,37].

CH_4 or CO_2 in the atmosphere is difficult to measure due of their light weight and small size. Devkota et al. [38,39] utilized a zeolitic imidazolate framework (ZIF) as a sensing material to fabricate a one-port DL-type SAW that showed a phase shift of the reflection signal depending on the concentrations of CO_2 and CH_4. The sensitivity of this sensor to CO_2 was greater than that to CH_4 because the amount of CH_4 adsorbed was smaller. In addition, it can be seen from this paper that the wave mode and wave velocity change depending on the coating thickness of the sensing material, and the sensitivity changes due to changes in wave characteristics. Optimization of the sensing layer thickness to improve the sensing performance is also a key point to consider when developing sensors.

Bahos et al. [40] demonstrated a sensor to detect acetone, ethanol, and ammonia markers related to diabetes mellitus by spin-coating ZIF-8 and ZIF-67 nanocrystals (pure and combined with gold nanoparticles (AuNPs)) as a SAW sensing material. Fig. 2 (b) shows the structures of ZIF-8 and ZIF-67. ZIF/AuNP layers synthesized using ZIF (with a higher surface area due to larger pore sizes and smaller crystal size characteristics) and AuNPs (with strong interaction characteristics with gas) showed improved sensitivity, limit of detection (LOD), and response time [39]. Furthermore, the sensor could detect and discriminate between acetone, ammonia, and ethanol using principal component analysis.

3.3 Graphene

Graphene oxide (GO) has high mechanical properties compared to other sensing materials. It exhibits good durability and has many hydrophilic groups, so it can adsorb a large amount of moisture, which is why it is often used in humidity sensors [41-44].

Jung et al. [41] fabricated a multi-frequency SAW humidity sensor that shares one GO sensing area and has three operational frequencies. By comparing the performances of three frequencies according to the level of relative humidity (RH), they identified an operational frequency that was favorable in the range of each RH level, showing that it is necessary to select the optimal operational frequency according to the range of measurement levels. Wang et al. [42] also demonstrated a DL-type SAW humidity sensor coated with GO using the drop-cast method. Utilizing well-matched circuits and software, the integrated SAW sensing system demonstrates a sensitivity of 3.33 kHz/%RH and high stability and repeatability over the range of 0 – 97.3%RH.

Fig. 2 (c) shows the gas adsorption and hydrogen bond formation diagrams of the porous graphene/PVDF film. Xu et al. [44] fabricated a highly selective SAW sensor for Dimethyl methylphosphonate (DMMP) using molecular imprinting technology to synthesize porous graphene/PVDF sensing material. Molecular imprinting technology is an option for improving sensor performance because it can show high selectivity for the analyte. The sensor demonstrated a high sensitivity of -1.407 kHz/ppm for DMMP due to the synergistic effect of porous graphene and PVDF, which improves the adsorption of DMMP by increasing the specific surface area.

Li et al. [27] fabricated a SAW-based gas sensor to detect NO_2 by spin-coating an MXene-activated sensing material on GO. The abundant functional groups of MXene and the unique multilayered structure of the MXene/GO sensitive layer enabled better adsorption of NO_2 gas, resulting in a high sensitivity of 260 Hz/ppm for NO_2.

Zhou et al. [28] demonstrated a SAW sensor that detects acetone with high sensitivity by forming a SiO_2 guiding layer in the sensing area and coating a graphene-sensing layer on top of the SiO_2. By using SiO_2 guiding layer to create a Love wave, the sensor performance was improved, and the sensitivity improved as the grain size of SiO_2 became smaller. Unlike conventional sensors that are dominated by the mass-loading effect, the sensing mechanism of this sensor is dominated by the viscoelastic effect of acetone adsorption on graphene.

3.4 Carbon Nanotubes

CNTs, which are classified as single-walled CNTs (SWCNTs) and multi-walled CNTs (MWCNTs), have interesting physical properties such as a high surface area, hollow structure, and chemical reactivity, making them popular sensing materials.

Wu et al. [46] reported that DL-SAW sensor using a p-hexafluoroisopropanol phenyl (HFIPPH)-functionalized MWCNT film as a sensing material showed very high selectivity to DMMP and also exhibited high sensitivity at the sub-ppm level. This was because the micropores in the sensing film adsorbed and transported gas molecules. In particular, the wet etching and dip coating methods used to integrate the sensing film into the bare SAW device ensured the uniformity of the sensing film, and the Hexagonal Boron Nitride (h-BN) layer exhibited good wettability to the HFIPPH-MWCNT solution, which prevented the coffee ring effect. Because functionalized MWCNTs used as sensing materials are highly conductive, the acoustoelectric effect dominates the sensing mechanism.

A two-port SAW sensor made by Penza et al. [26] used an nanocomposite film of MWCNTs as the sensing material, and it was confirmed through experiments that the sensor exhibited selectivity for ethanol and methanol. The experiments confirmed that the higher the operating frequency and larger the amount of sensing material, the higher the sensitivity. However, in general, high operating frequency and signal noise have a trade-off relationship. In the case of ethanol, the nonlinearity of the frequency shift response with the gas concentration showed that the mass-loading effect, as well as the viscoelastic and acoustoelectric effects, affected the frequency shift.

Vizireanu et al. [47] demonstrated a SAW sensor for H_2 and CH_4 detection by modifying the surface chemistry of carbon nanowalls (CNWs) using hydrogen plasma treatment, which improved the sensing ability. Fig. 2 (d) shows SEM images of the CNWs before and after plasma treatment, and it can be seen that the morphology changed after plasma treatment. This change enhances the adsorption capacities for H_2 and CH_4. Thus, the sensitivity and LOD improved compared to those of the SAW sensor before plasma treatment.

3.5 Noble Metal Nanoparticles

Because of their large surface area and capability for gas molecule adsorption, metal NPs are of interest as sensing materials.

Asri et al. [48] demonstrated a CO_2 detector with excellent performance based on nanostructured silicon combined with a SAW sensor. A metal-assisted chemical etching (MACE) method was utilized to form a nanostructured silicon layer, and the sensing material was coupled to the SAW sensor based on analytically

optimal sensing material dimensions through FEA. Notably, the sensor operates at a low frequency of 19.96 MHz but shows a frequency shift of 4.621 kHz at a CO_2 concentration of 2000 ppm, which is comparable or superior to that of other CO_2 sensors.

Kus et al. [49] fabricated a SAW device by the drop-casting method using Au nanorods (AuNRs) and Au nanocubes (AgNCs), which have the advantage of increasing interaction sites owing to their high surface-to-volume ratio, and calix [4] arene, which interacts well with volatile organic compounds (VOCs). The synergistic effect of the metal nanomaterial and calix [4] arene improved the sensing performance for VOCs by six to eight times compared to that of the individual materials.

Scarisoreanu et al. [50] fabricated CH_4 sensors by spin-coating sensing materials, such as W&V:TiO_2 and W:TiO_2, with metal NPs, such as Ag, Pt, and Pd, on SAW devices using a Polyethylenimine (PEI) polymer as a deposition matrix. The sensor was evaluated for CH_4 by categorizing the sensing films as S1 – S9 according to the combination of W or W and V doping and the loading of Ag, Pt, and Pd NPs. Fig. 2 (e) shows the TEM image of the TWV-7-0@Ag. The specific surface area was increased by metal doping and the loading of metal NPs, indicating that the sensor performance increased. The authors demonstrated the frequency shift for CH_4 in S1 – S9 films, and the highest sensitivity of 1.79 Hz/ppm and LOD of 17 ppm was observed for S9-TWV-7-1-Pd-PEI.

3.6 Polymers

Polymers have the advantages of low cost and ease of fabrication as sensing materials. Kesuma et al. [51] fabricated a one-port SAW sensor using the photoresist polymer S1805 as a humidity-sensing material. S1805 has the advantage of being a photoresist capable of adsorbing humidity and can be deposited on the desired area relatively easily by photolithography. Utilizing photolithography to improve the performance of a one-port SAW sensor by depositing the sensing material only on the reflector area, the humidity sensor exhibited a sensitivity of 155.6 Hz/%RH.

Memon et al. [29] fabricated a SAW humidity sensor using fluorinated polyimide (PI) as the sensing material and demonstrated a high sensitivity of 4.15 kHz/%RH despite the hydrophobic nature of PI. Unlike conventional sensors, which show a negative frequency shift owing to the mass loading effect when the RH increases, they tend to show a positive frequency shift when the RH increases owing to the viscoelastic effect due to the hardening phenomenon caused by the water absorption of the PI.

Fig. 2 (f) shows chemical structure of sensing materials: polyhedral oligomeric silsesquioxane (POSS), 1-benzyl-3-phenylthiourea (TU-1) and 1-ethyl-3-(4 fluorobenzyl) thiourea (TU-2). Kim et al. [52] demonstrated a sensor that detects nerve agents using drop-casted POSS-, TU-1, and TU-2-based polymer sensing materials onto a DL-SAW. It was experimentally confirmed that POSS-based polymers have a higher sensitivity because fluorinated alcohols or fluorinated phenolic functional groups maximize hydrogen bonding.

Gas sensors that utilize the photoconductive properties of sensing materials are another possibility. Jakubik et al. [30] demonstrated a light-activated SAW sensor that detects changes in DMMP by utilizing photoconductive polymer films such as (rr)P3HT (regio-regular Poly-3-hexylthiophene) and SilPEG1.4 as the sensing materials. In particular, the sensor showed high sensitivity to DMMP owing to its enhanced DMMP adsorption ability and increased acoustoelectric interaction upon light activation.

4. INTEGRATION METHODS

4.1 Spin Coating

Spin coating allows for the rapid and simple formation of uniform thin films. This process involves dropping a solution onto a rotating substrate at high speeds, utilizing centrifugal force to evenly spread the solution across the surface of the substrate [53]. The thickness and uniformity of the thin film can be controlled by adjusting factors such as the amount of solution, viscosity, spin coater rotation speed, and spin time [53-56]. Fig. 3 (a) shows the spin-coating process and the variation in film thickness depending on the rotation speed [57].

The advantages of spin coating include its simplicity and ability to form thin films over a large area at a low cost [27,32,34,40,50]. Using a simple technique, one can distinguish between areas that one wants to coat with a sensing film and those that one does not. It is possible to protect areas that do not want to be coated with adhesive tape [29]. If the sensing material is a photoresist, the sensing film can only be coated in the desired area by photolithography after spin coating [51]. Despite the simplicity of the process, which allows the formation of high-performance thin films, one drawback is the lack of material efficiency. Through high-speed rotation, 95 – 98% of the solution distributed on the substrate is discarded outside the substrate [54]. Additionally, drying the applied solution can take several hours, making the process inefficient in terms of overall time.

4.2 Dip Coating

Dip-coating is another thin-film deposition method used for

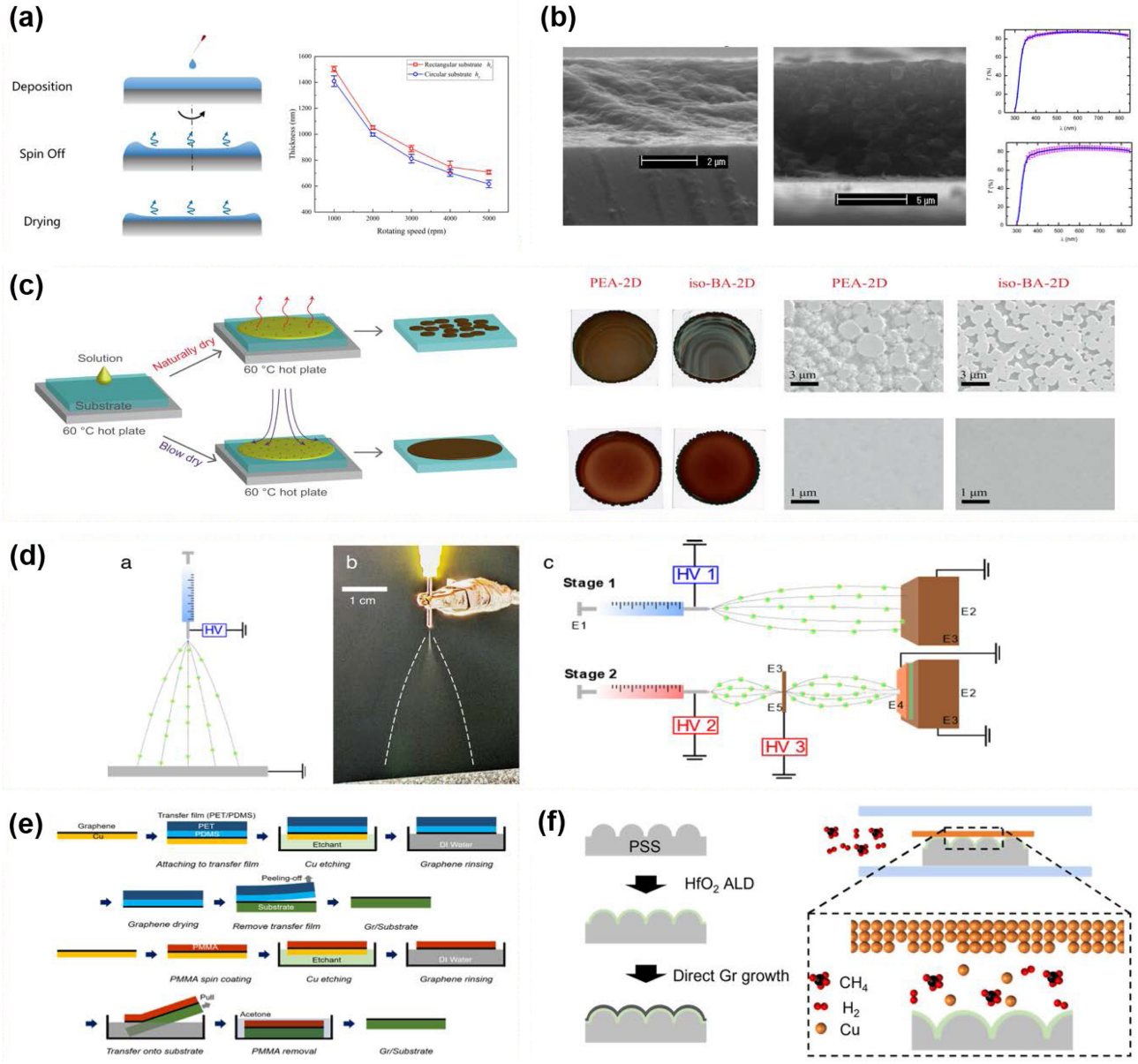

Fig. 3. Integration methods for sensing material: (a) Schematic diagram of spin-coating. Reprinted with permission from Ref. [57]. Copyright (2021) MDPI. (b) SEM images of dip coated. Reprinted with permission from Ref. [59]. Copyright (2018) MDPI. (c) Schematic diagram of drop-casting. Reprinted with permission from Ref. [62]. Copyright (2020) Nature. (d) Schematic of electrospray deposition. Reprinted with permission from Ref. [65]. Copyright (2023) Nature. (e) Schematic diagram of the transfer process. Reprinted with permission from Ref. [69]. Copyright (2022) MDPI. (f) Schematic diagram of direct growth. Reprinted with permission from Ref. [72]. Copyright (2023) MDPI.

SAW device fabrication and integration [46]. This process involves immersing the substrate in a solution and slowly withdrawing it, allowing the solution to thinly coat the substrate surface. Similar to spin coating, the thickness of the film is determined by factors such as surface tension, gravity, viscosity, and deposition time of the dip-coating process [56,58]. In addition, the thickness of the sensing film can be controlled by varying the number of dip-coating cycles [37,38]. Fig. 3 (b) shows SEM images corresponding to different withdrawal speeds (10 and 20 cm/min) and the average transmittance of the deposited films at each withdrawal speed [59].

Dip coating allows for deposition on large-area substrates and can be applied to substrates with complex shapes. It is simpler in terms of equipment and more cost-efficient than spin coating. However, the uniformity of the thin film decreases depending on the viscosity of the solution [60]. This renders this method unsuitable for the formation of thick films through repeated depositions.

4.3 Drop Casting

Drop casting is a simple and cost-effective method for forming uniform films [44,52]. In this process, a small amount of the desired solution is dropped onto the electrode surface and allowed to spread naturally as the solvent evaporates and dries at room temperature or under controlled conditions to form a thin film [56,61]. During this process, the coffee-ring effect may occur, where the solute concentrates at the edges as the liquid evaporates [42]. Therefore, additional control is required to achieve a uniform coating. As shown in Fig. 3 (c), the drying method, such as natural drying or N_2 drying, affects the morphology of the film. The images show films dried naturally, and the bottom images show films dried using N_2 blowing. N_2 drying generally resulted in a uniform, dense, and smooth surface [62]. In addition, the coffee-ring effect can be reduced by making the substrate hydrophilic through plasma treatment or by synthesizing the sensing material with another solution to make it aqueous [43,49].

However, this method's drawback is that it is difficult to achieve a uniform coating over large areas. To address this, Eslamian et al. [63] improved the spread of water droplets and the uniformity of films by applying ultrasonic vibration to substrates coated with fluorine-doped tin oxide (FTO). Consequently, the films deposited on FTO-coated substrates exhibited improved coverage.

4.4 Electrospray Deposition

The fabrication method of integrating sensing material using electrospray is primarily used to form nanostructured thin films on substrates. This allows for the formation of thin films with high uniformity and precise deposition [64]. The flow rate of the sprayed liquid is controlled using a syringe pump, and the voltage is adjusted, making it a simple and easy-to-operate method. As shown in Fig. 3 (d), when a very high voltage was applied to the liquid droplets, they were atomized. If the electrostatic repulsion exceeds the surface tension, which is known as the Rayleigh limit, the droplets break down into fine particles [65]. Subsequently, as the particles are charged, they follow the electric field, during which the solvent evaporates, and the particles are uniformly deposited onto the substrate [41,66].

This method is particularly advantageous for SAW applications because it allows precise control over the deposition of functional materials such as polymers, nanoparticles, and bioactive molecules. This contributes to optimizing the device performance by effectively tuning the acoustic properties of SAW sensors or enhancing their sensing capabilities. Electrospray deposition (ESD) can be applied to many processes in modern materials technology, microelectronics, and nanotechnology, as well as in the manufacturing of scientific instruments [67].

4.5 Transfer Method

The transfer method is used to move specific materials or films onto a substrate by physically transferring thin films or materials previously fabricated using another process [68]. Fig. 3 (e) shows the method for transferring graphene onto the desired substrate. Yoon et al. [69] coated a sensing material onto a Cu foil with low solubility, followed by laminating a transfer film on top of the sensing material. Using a specific solution, Cu was removed, and the structure adhered to the desired substrate. The transfer film was then peeled off using a dry or wet transfer process.

This process is applicable to various substrates, making it suitable for a wide range of applications, such as sensors and electronic devices [28,70]. However, residues from these materials may remain on the surface of the sensing material, potentially degrading its properties. Additionally, care must be taken during the transfer process because defects such as wrinkles, cracks, or tears may occur, leading to performance degradation [71].

4.6 Direct Growth

Direct growth method allows the desired material to be formed directly on a substrate without the need for a transfer process. As shown in Fig. 3 (f), this technique typically uses chemical vapor deposition (CVD) to grow materials directly at fixed locations, resulting in high-quality coatings [72].

Unlike the transfer method, direct growth avoids performance-degrading defects such as wrinkles, tears, and residues, enabling the formation of uniform and high-quality thin films without impurities, which is why it is widely used [47,73]. However, because CVD requires high temperatures, its application to substrates sensitive to high temperatures may be challenging. Additionally, the growth of the desired material may only be possible on specific substrates; therefore, compatibility must be considered.

5. SENSING APPLICATIONS

SAW technology has been widely utilized in various sensors owing to its various advantages, such as miniaturization, high sensitivity, fast recovery, and quick response time. For chemical

sensors, the target substance is essential, and the sensor must be able to detect low concentrations of the material, even under limited conditions. The high sensitivity and real-time monitoring capabilities of SAW sensors make them particularly well-suited for gas-sensing applications, and numerous studies have highlighted their effectiveness in this area.

5.1 Gas (VOCs) Sensing

Various studies have reported the detection of VOCs using SAW [49,74]. VOCs are organic compounds that can easily evaporate into the atmosphere; common examples include acetone, toluene, and benzene. These VOCs can contribute to air pollution and negatively affect human health, leading to increased interest in controlling VOC concentrations for real-time environmental monitoring [75-78].

Sensor coating technologies utilizing nanomaterials have advanced [42,66]. Materials such as graphene, metal oxides, and 2D materials significantly enhance sensitivity and selectivity [30,41,42,47]. Fig. 4 (a) shows the use of ZIF nanocrystals for

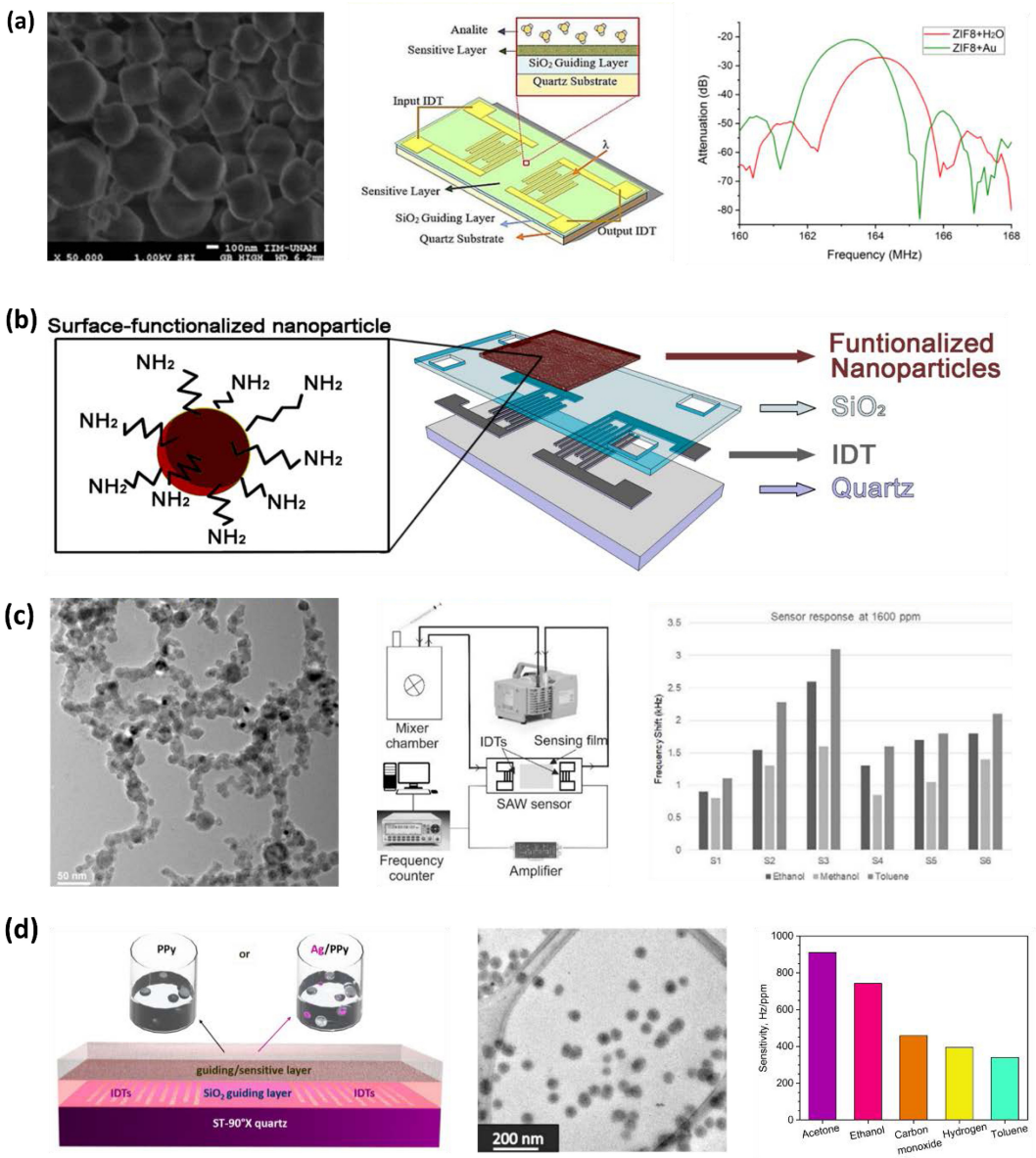

Fig. 4. VOC Sensing: (a) Schematic representation of Love-wave sensor and synthesis and characterization of ZIF-67 layer. Reprinted with permission from Ref. [40]. Copyright (2018) MDPI. (b) Love-wave sensor with a functionalized nanoparticle sensing layer. Reprinted with permission from Ref. [80]. Copyright (2017) MDPI. (c) TEM image of nanoparticles and experimental results for VOC sensing. Reprinted with permission from Ref. [81]. Copyright (2018) MDPI. (d) Love-wave SAW sensor with polypyrrole nanoparticles and sensitivity of VOCs. Reprinted with permission from Ref. [82]. Copyright (2020) MDPI.

detection of VOCs [40]. When ZIF binds to VOCs such as acetone, it causes a frequency shift in the SAW sensor, which is analyzed to detect VOCs.

Šetka et al. [79] developed highly sensitive Love-mode SAW sensors by incorporating cadmium telluride/polypyrrole nanocomposites that demonstrated high sensitivity to VOCs. The results showed the highest sensitivity to acetone, confirming that the sensing composite area effectively adsorbed VOCs.

Fig. 4 (b) shows a Love-wave SAW sensor, where a sensing material is deposited using the spin-coating method, allowing a larger sensing area [80]. The research group presented a method for detecting VOCs using Love-wave SAW sensors based on amino-functionalized iron oxide nanoparticles. They demonstrated the high sensitivity and fast response times of the sensor for organic solvents such as butanol, isopropanol, toluene, and xylene. The sensor response varied depending on the solvent concentration, with detection limits as low as 1, 2, 3, and 5 ppm for butanol, isopropanol, toluene, and xylene, respectively. This Love-wave sensor offers high sensitivity and selectivity at a low cost and shows great potential for industrial and environmental applications.

Fig. 4 (c) illustrates the frequency changes for various VOC gases, showing that many studies have focused on highly sensitive SAW sensors using nanoparticle coatings. The research group analyzed SAW sensors with polymer-sensing layers containing Fe_3O_4 nanoparticles of various sizes and concentrations to detect VOCs. The results showed that increasing the nanoparticle concentration improved the sensor sensitivity, and smaller nanoparticles provided better performance. The SAW sensor with 7 nm nanoparticles had a short response time of approximately 9 seconds for ethanol and a limit of detection of 65 ppm, which was approximately five times better than that of the sensor using the polymer alone. This demonstrates that the nanoparticle size and concentration significantly affect sensor performance [81].

Fig. 4 (d) illustrates the Love-wave SAW sensor schematic with polypyrrole nanoparticles image and the experimental result. The research group developed Love-wave sensors with silver-modified polypyrrole nanoparticles for VOC detection. This study demonstrated high sensitivity and fast response times for VOCs, with a limit of detection as low as 3 ppb for acetone. The sensor operates at room temperature, and the silver-modified polypyrrole nanoparticles enhance the gas-solid interactions, improving the detection performance. These sensors show potential for applications in air quality monitoring, food assessment, and disease diagnosis via breath analysis [82].

Kannan et al. [83] conducted a study using an SAW sensor coated with Carbowax-1000 to detect 2,4-dinitrotoluene (DNT) vapor. DNT is found in explosives such as landmines and forms a chemical signature in vapor form at very low concentrations. Highly sensitive sensors are required for accurate detection. The authors used a 150 MHz SAW device with Carbowax-1000 as a chemical interface. The results demonstrated that the sensing material had excellent adsorption properties for DNT vapor and exhibited a linear response in the ppb concentration range.

There have been active reports on sensors capable of real-time detection of harmful agents through various sensing materials and binding mechanisms between the sensor and target substances.

5.2 Chemical Sensing

SAW sensors are also suitable for detecting harmful gases such as CO_2, CO, and NO_x [84-87]. One of the key strengths of SAW is their high sensitivity to small mass changes on the surface, allowing for the precise detection of even trace amounts of gas molecules. This makes it ideal for detecting harmful gases at extremely low concentrations, which is crucial for environmental monitoring and industrial safety management. In addition, SAW sensors offer fast response and recovery times because they can instantly detect frequency shifts caused by the adsorption or desorption of gases from the surface. These real-time monitoring capabilities make SAW sensors well-suited for quickly detecting gases such as CO_2, CO, and NO_x and tracking their concentrations in real time. The high sensitivity and rapid response of SAW sensors, combined with their ability to be functionalized with various materials, make them highly effective harmful gas sensors.

Lim et al. [85] developed a 440 MHz wireless and passive SAW-based multi-gas sensor for the simultaneous detection of CO_2 and NO_2. The sensor included a CO_2-sensitive film (Teflon AF 2400) and an NO_2-sensitive film (Indium Tin Oxide, ITO), which detected changes in the SAW velocity due to gas adsorption. The sensitivity was measured at 2.12 °C/ppm for CO_2 and 51.5 °C/ppm for NO_2. The sensor also features temperature compensation to minimize the effect of temperature variations during the gas sensitivity evaluation.

Nikolaev et al. [84] fabricated and investigated ZnO-nanorod-based resistive and SAW CO gas sensors. Their study focused on developing resistive sensors using ZnO nanorod arrays synthesized by pulsed laser deposition at a high argon pressure to detect CO. They constructed several resistive CO sensors and analyzed their resistive properties. The results showed that the resistance of the ZnO nanorods changed linearly with CO concentration. Additionally, the reflection coefficient of the SAW sensor varied with the CO concentration, demonstrating its potential to detect small amounts

of CO gas.

Wen et al. [86] developed a novel NO_2 gas sensor by using a dual-track SAW device. Their research team applied a porous tungsten trioxide (WO_3) film in the sensitive area of a SAW device to detect NO_2 gas. Experimental results showed excellent response characteristics for NO_2 concentrations between 0.5 ppm and 10 ppm. The dual-track design effectively eliminated external perturbations caused by environmental factors. The sensor also demonstrated good reproducibility and stability, indicating its potential for long-term use and its ability to detect various gases.

5.3 Biological Sensing

SAW has high sensitivity and is capable of detecting even the smallest changes in surface mass, which gives it a significant advantage in detecting tiny biomarkers such as proteins and DNA [88-91]. Additionally, SAW devices enable real-time monitoring, making them advantageous in situations where immediate detection and analysis of biological signals are required. For example, it plays an important role in detecting biomarkers in body fluids and monitoring environmental changes in living systems.

Hur et al. [90] developed shear horizontal SAW (SH-SAW) sensors for detecting DNA hybridization. They conducted DNA hybridization experiments using 15-meroligonucleotides on gold-coated DLs of the SAW device. The sensors operated at 100 MHz and detected the frequency changes caused by the mass-loading effect from the hybridization between the target DNA and the immobilized probe DNA. The experiments showed that the sensor responded to DNA hybridization with a sensitivity of up to 1.55 ng/ml/Hz, and 6-Mercapto-1-hexanol was used as a blocking layer to prevent nonspecific binding.

Klumpers et al. [88] used an SH-SAW biosensor to monitor protein-protein interactions in real-time. The research group analyzed the interaction between Ras GTP-binding proteins and their effector protein Nore1A. Their study showed that Nore1A binds only to the active K-Ras-GppNHp complex, and not to the inactive K-Ras-GDP. The binding strength decreased as the salt concentration increased.

Rydosz [92] analyzed acetone detection sensors as a potential tool for non-invasive diabetes monitoring. By analyzing VOCs in human exhaled breath resulting from metabolic changes or pathological disorders, they aimed to detect elevated acetone levels in the breath of diabetic patients. This study focused on recent advancements in gas sensor technology for acetone detection, with the goal of developing non-invasive diagnostic tools that could replace the current invasive methods used for blood sugar measurement in diabetes patients.

Das et al. [93] introduced a detachable SAW immunosensor for the rapid detection of diabetic retinopathy (DR). They analyzed the protein biomarker Lipocalin 1 (LCN1) in human tear samples, and the device enabled early diagnosis of DR. The reusable SAW microchip achieved 99% accuracy within 3 min, and a clinical test involving 10 participants demonstrated high sensitivity and accuracy, with results consistent with those of the traditional ELISA test.

Gray et al. [94] conducted a study using dual-channel SAW biosensors for an ultra-rapid and highly sensitive HIV diagnosis. They developed a small laboratory prototype using low-cost smartphone components and employed dual-channel biochips to detect HIV antibodies. In a pilot clinical study involving 133 patient samples, they achieved 100% sensitivity and specificity for antibody detection. Notably, anti-gp41 antibodies were detected within 60 s, and the biochip electronic readout provided rapid and accurate results.

5.4 Humidity Sensing

Humidity is one of the factors that affects our daily lives. It is a critical variable in various environmental monitoring and industrial fields. Beyond agriculture and meteorology, humidity has emerged as a key factor in monitoring human respiration, indoor air quality, and viral transmission [95,96]. Consequently, the demand for humidity sensors has been increasing across various sectors, and in specialized fields, there is a growing need for sensors that are accurate, precise, and exhibit fast response characteristics.

Wu et al. [97] developed a highly sensitive nanomaterial-based SAW humidity sensor. They designed a humidity sensor using a 128° YX-$LiNbO_3$-based SAW resonator operating at 145 MHz. To eliminate the external temperature fluctuations, a dual-DL configuration was introduced. For selective coating, camphor sulfonic acid-doped polyaniline nanofibers, which possess a high surface-to-volume ratio, were used to enhance the sensitivity. The humidity sensor measured various RH levels between 5% and 90%, exhibited excellent sensitivity and short-term repeatability.

Fig. 5 (a) shows schematic diagram of humidity sensing experiment and its results [98]. Jakubik et al. investigated the humidity-sensing properties of regioregular rr-P3HT (poly-3-hexylthiophene) polymer films using SAW sensors fabricated on 128° YX-$LiNbO_3$ and ST-quartz piezoelectric substrates. The performance of the sensor improved with increasing rr-P3HT film thickness, with a phase shift of approximately −8.2° measured at 60% RH for a 240 nm thick polymer membrane. The sensor exhibited fast and linear responses over the RH range of 5 – 60%, and the polymer

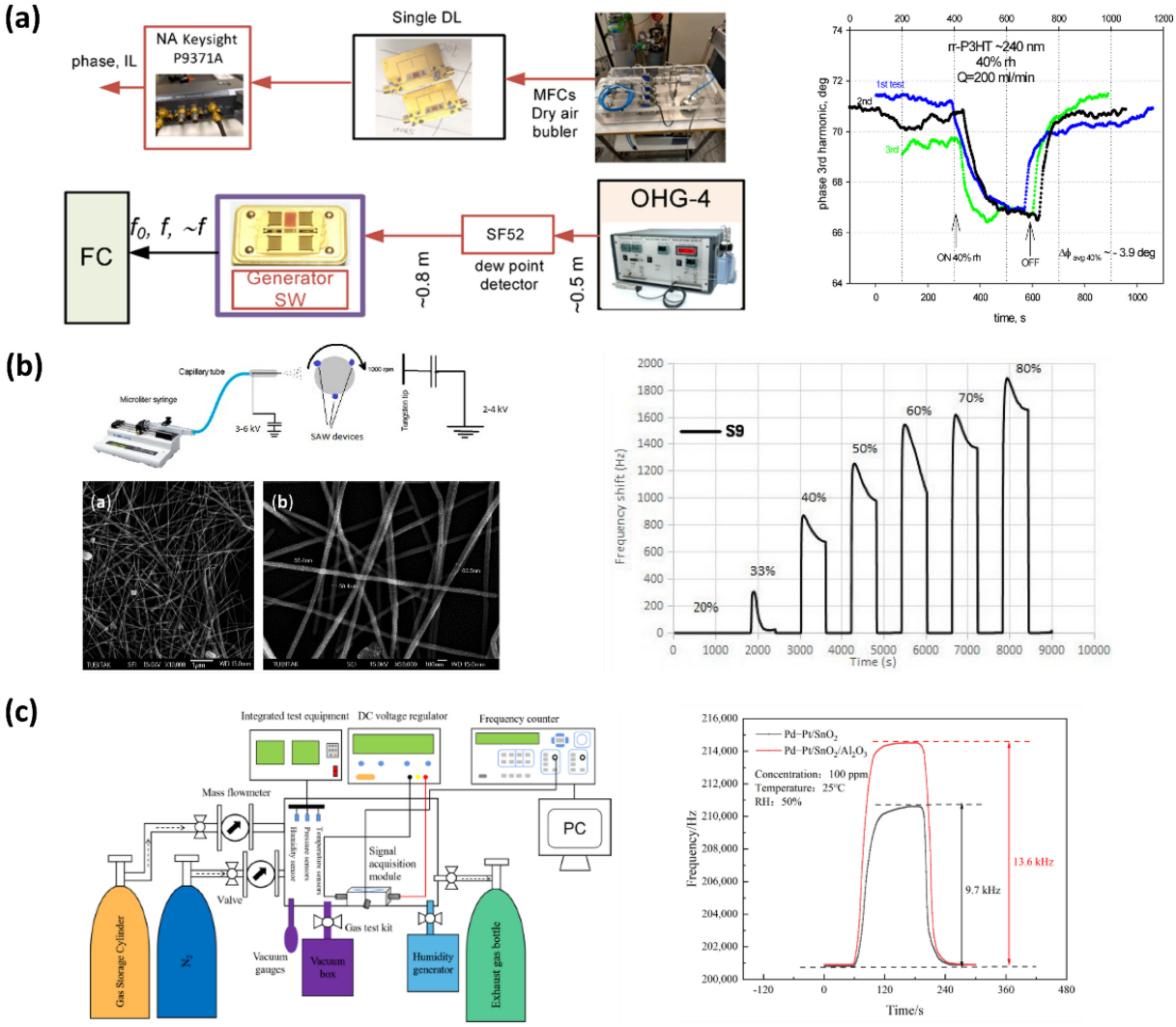

Fig. 5. Humidity sensing: (a) Schematic diagram of experimental setup and humidity sensing result. Reprinted with permission from Ref. [98]. Copyright (2024) MDPI. (b) Schematic diagram of the experimental setup; SEM images of silver nanowire and experimental result. Reprinted with permission from Ref. [99]. Copyright (2016) MDPI. (c) Schematic diagram of test setup and experimental result. Reprinted with permission from Ref. [100]. Copyright (2023) MDPI.

layer was fabricated using a low-cost coating method. The sensor demonstrated much faster response times than commercially available humidity sensors and showed potential for use in low-to medium-range humidity-sensing applications.

Fig. 5 (b) shows the silver nanowire and humidity-sensing result [99]. Irani et al. enhanced the sensitivity of SAW humidity sensors with silver nanowires (AgNWs) coated using ESD. They synthesized AgNWs with an average length of 15 μm and a diameter of 60 nm and coated them onto 433 MHz Rayleigh-SAW devices. Their investigation showed that increasing the coating thickness improved sensor sensitivity, with a maximum frequency shift of 262 kHz. At 80% RH, the sensor demonstrated three times higher sensitivity than that of the uncoated sensor.

Fig. 5 (c) illustrates the experimental setup and results [100]. Yang et al. studied the gas and humidity sensitivities of a high-frequency SAW CO gas sensor based on a noble metal-modified metal oxide (Pd-Pt/SnO_2/Al_2O_3) thin film. Their research team conducted experiments at 25 °C and 50% RH, testing CO concentrations ranging from 10 to 100 ppm. The sensor based on Pd-Pt/SnO_2/Al_2O_3 films showed a high-frequency response of 13.6 kHz at 100 ppm Co concentration, and the frequency response decreased as humidity increased from 25% to 75%. The sensor demonstrated an average response time of 33.4 s and an average recovery time of 37.2 s, demonstrating excellent performance in detecting CO gas under varying humidity conditions.

Le et al. [101] developed a high-performance humidity sensor using an aluminum nitride/silicon (AlN/Si) layered structure and a GO sensing layer. They applied the GO thin film, and the

sensitivity of the humidity sensor was significantly increased, reaching 42.08 kHz/RH% at RH levels above 80%. The sensor performed well in both low humidity (≤10% RH) and high humidity (≥90% RH) ranges, demonstrating low hysteresis, excellent repeatability, and long-term stability. Also, the AlN/Si layered structure greatly improved the thermal stability, and the temperature coefficient of frequency of the sensor was reduced to -22.1 ppm/°C, which is much lower than previously reported sensors.

6. CONCLUSIONS

In this review, we demonstrated that SAW sensors offer versatile advantages, including miniaturization, compatibility with semiconductor processes, fast response and recovery times, high sensitivity, and low power consumption, which make them suitable for a wide range of sensing applications. In addition, we demonstrate how SAW sensors are evolving alongside the evolution of nanomaterials in areas such as environmental monitoring, gas detection, and humidity sensing. We also emphasize the importance of the sensing materials and integration methods in the development of SAW sensors.

Recent studies have shown that sensors incorporating nanomaterials, such as ZnO, ZIF, graphene, and functional materials that strongly interact with the analyte, show high sensitivity and selectivity. Simultaneously, an optimal integration method, such as ESD or CVD, is necessary to integrate a uniform and dense sensing film into the device. The numerous examples of SAW sensor applications presented in this paper demonstrate that the sensing materials are critical for the desired application.

There are many possibilities for improving SAW sensors, including sensing materials, integration methods, and design. To develop robust sensors with enhanced performances, ongoing research on sensor reliability is essential. This includes exploring new sensing materials, improving sensor durability in high-temperature and extreme environments, and enhancing sensor accuracy.

ACKNOWLEDGMENT

This research was funded by the Korea Institute of Industrial Technology as “Development of core technology for smart sensing and digital medical process to support medical surgical field diagnosis” (KITECH EH-24-0005) and by the National Research Foundation of Korea (NRF), funded by the Ministry of Science and ICT of Korea (RS-2024-00346135).

REFERENCES

[1] C. K. Kent, N. Ramakrishnan, and H. P. Kesuma, “Advancements in One-Port Surface Acoustic Wave (SAW) Resonators for Sensing Applications: A Review”, *IEEE Sens. J.*, Vol. 24, No. 11, pp. 17337-17352, 2024.

[2] B. E. Rapp, A. Voigt, M. Dirschka, M. Rapp, and K. Länge, “Surface Acoustic Wave Resonator Chip Setup for the Elimination of Interfering Conductivity Responses”, *Micromachines*, Vol. 15, No. 4, p. 501, 2024.

[3] H. Nazemi, A. Joseph, J. Park, and A. Emadi, “Advanced micro-and nano-gas sensor technology: A review”, *Sensors*, Vol. 19, No. 6, p. 1285, 2019.

[4] D. Mandal and S. Banerjee, “Surface acoustic wave (SAW) sensors: Physics, materials, and applications”, *Sensors*, Vol. 22, No. 3, p. 820, 2022.

[5] K. Lee, W. Wang, T. Kim, and S. Yang, “A novel 440 MHz wireless SAW microsensor integrated with pressure–temperature sensors and ID tag”, *J. Micromech. Microeng.*, Vol. 17, No. 3, p. 515, 2007.

[6] W. Buff, F. Plath, O. Schmeckebier, M. Rusko, T. Vandahl, H. Luck, F. Moller, and D. C. Malocha, “Remote sensor system using passive SAW sensors”, *Proc. of IEEE Ultrasonics Symposium*, pp. 585-588, Cannes, France, 1994.

[7] A. Barani, H. Paktinat, M. Janmaleki, A. Mohammadi, P. Mosaddegh, A. Fadaei-Tehrani, and A. Sanati-Nezhad, “Microfluidic integrated acoustic waving for manipulation of cells and molecules”, *Biosens. Bioelectron.*, Vol. 85, pp. 714-725, 2016.

[8] G. Destgeer and H. J. Sung, “Recent advances in microfluidic actuation and micro-object manipulation via surface acoustic waves”, *Lab. Chip*, Vol. 15, No. 13, pp. 2722-2738, 2015.

[9] J. Devkota, P. R. Ohodnicki, and D. W. Greve, “SAW Sensors for Chemical Vapors and Gases”, *Sensors*, Vol. 17, No. 4, p. 801, 2017.

[10] M. Hoummady, A. Campitelli, and W. Wlodarski, “Acoustic wave sensors: Design, sensing mechanisms and applications”, *Smart Mater. Struct.*, Vol. 6, No. 6, p. 647, 1997.

[11] F. Della Lucia, P. Zambrozi Jr, F. Frazatto, M. Piazzetta, and A. Gobbi, “Design, fabrication and characterization of SAW pressure sensors for offshore oil and gas exploration”, *Sens. Actuators A Phys.*, Vol. 222, pp. 322-328, 2015.

[12] H. Zhang, P. Chen, L. Yang, H. Wang, and Z. Zhu, “Fabrication of Surface Acoustic Wave Biosensors Using Nanomaterials for Biological Monitoring”, *Nanomanufacturing*, Vol. 4, No. 3, pp. 159-172, 2024.

[13] B. A. Auld, *Acoustic fields and waves in solids*, New York, John Wiley & Sons, NY, pp. 1-423, 1973.

[14] F. Hadj-Larbi and R. Serhane, “Sezawa SAW devices: Review of numerical-experimental studies and recent applications”, *Sens. Actuators A Phys.*, Vol. 292, pp. 169-197, 2019.

[15] L. Y. Yeo and J. R. Friend, “Surface acoustic wave microfluidics”, *Annu. Rev. Fluid Mech.*, Vol. 46, No. 1, pp. 379-406, 2014.

[16] C. Caliendo, P. Verardi, E. Verona, A. D'Amico, C. Di

Natale, G. Saggio, M. Serafini, R. Paolesse, and S. E. Huq, "Advances in SAW-based gas sensors", *Smart Mater. Struct.*, Vol. 6, No. 6, p. 689, 1997.
[17] B. Liu, X. Chen, H. Cai, M. M. Ali, X. Tian, L. Tao, Y. Yang, and T. Ren, "Surface acoustic wave devices for sensor applications", *J. Semicond.*, Vol. 37, No. 2, p. 021001, 2016.
[18] T. Hoang, "SAW parameters analysis and equivalent circuit of SAW device", in Acoustic Waves-From Microdevices to Helioseismology, M. G. Beghi, Eds. InTech, London, pp. 443-483, 2011.
[19] A. Kang, C. Zhang, X. Ji, T. Han, R. Li, and X. Li, "SAW-RFID enabled temperature sensor", *Sens. Actuators A Phys.*, Vol. 201, pp. 105-113, 2013.
[20] R. M. White and F. W. Voltmer, "Direct piezoelectric coupling to surface elastic waves", *Appl. Phys. Lett.*, Vol. 7, No. 12, pp. 314-316, 1965.
[21] Z. Awang, "Gas sensors: A review", *Sens. Transducers*, Vol. 168, No. 4, pp. 61-75, 2014.
[22] D. S. Ballantine, R. M. White, S. J. Martin, A. J. Ricco, E. T. Zellers, G. C. Frye, and H. Wohltjen, *Acoustic wave sensors: theory, design and physico-chemical applications*, Academic Press, San Diego, CA, pp. 1-430, 1996.
[23] A. K. Namdeo and H. B. Nemade, "Extraction of electrical equivalent circuit of one port SAW resonator using FEM-based simulation", *Proc. of the 2015 COMSOL Conference*, pp. 1-6, Pune, India, 2015.
[24] M. Penza, F. Antolini, and M. V. Antisari, "Carbon nanotubes as SAW chemical sensors materials", *Sens. Actuators B Chem.*, Vol. 100, No. 1-2, pp. 47-59, 2004.
[25] M. Pasternak, "Applicability of different SAW oscillators' topologies for high frequency gas sensors construction", *Acta Phys. Pol. A*, Vol. 118, No. 6, pp. 1232-1234, 2010.
[26] M. Penza, R. Rossi, M. Alvisi, P. Aversa, G. Cassano, D. Suriano, M. Benetti, D. Cannata, F. Di Pietrantonio, and E. Verona, "SAW Gas sensors with carbon nanotubes films", *Proc. of 2008 IEEE Ultrasonics Symposium*, pp. 1850-1853, Beijing, China, 2008.
[27] X. Li, Y. Feng, J. Long, H. Lv, Y. Guo, and X. Zu, "MXene-activated graphene oxide enhancing NO_2 capture and detection of surface acoustic wave sensors", *Sens. Actuators B Chem.*, Vol. 401, p. 135006, 2024.
[28] H. Zhou, S. G. Ramaraj, K. Ma, M. S. Sarker, Z. Liao, S. Tang, H. Yamahara, and H. Tabata, "Real-time detection of acetone gas molecules at ppt levels in an air atmosphere using a partially suspended graphene surface acoustic wave skin gas sensor", *Nanoscale Adv.*, Vol. 5, No. 24, pp. 6999-7008, 2023.
[29] M. M. Memon, Y. Hongyuan, S. Pan, T. Wang, and W. Zhang, "Surface acoustic wave humidity sensor based on hydrophobic polymer film", *J. Electron. Mater.*, Vol. 51, No. 10, pp. 5627-5634, 2022.
[30] W. Jakubik, J. Wrotniak, A. Kaźmierczak-Bałata, A. Stolarczyk, and P. Powroźnik, "Light-activated SAW sensor structures with photoconductive polymer films for DMMP detection", *Sens. Actuators B Chem.*, Vol. 384, p. 133597, 2023.
[31] S. Das, K. Girija, A. Debnath, and R. Vatsa, "Enhanced NO_2 and SO_2 sensor response under ambient conditions by polyol synthesized Ni doped SnO_2 nanoparticles", *J. Alloys Compd.*, Vol. 854, p. 157276, 2021.
[32] L. Zhou, Z. Hu, P. Wang, N. Gao, B. Zhai, M. Ouyang, G. Zhang, B. Chen, J. Luo, S. Jiang, H. Y. Li, and H. Liu, "Enhanced NO_2 sensitivity of SnO_2 SAW gas sensors by facet engineering", *Sens. Actuators B Chem.*, Vol. 361, p. 131735, 2022.
[33] L. Shu, T. Jiang, Y. Xia, X. Wang, D. Yan, and W. Wu, "The Investigation of a SAW Oxygen Gas Sensor Operated at Room Temperature, Based on Nanostructured ZnxFeyO Films", *Sensors*, Vol. 19, No. 13, p. 3025, 2019.
[34] K. J. Lee, H. Oh, M. Jo, K. Lee, and S. S. Yang, "An ultraviolet sensor using spin–coated ZnO nanoparticles based on surface acoustic waves", *Microelectron. Eng.*, Vol. 111, pp. 105-109, 2013.
[35] W. Water and R.-Y. Jhao, "Application of ZnO nanorods synthesized on 64° Y-cut $LiNbO_3$ to surface acoustic wave ultraviolet photodetector", *Sens. Actuators B Chem.*, Vol. 173, pp. 310-315, 2012.
[36] L. E. Kreno, K. Leong, O. K. Farha, M. Allendorf, R. P. Van Duyne, and J. T. Hupp, "Metal–organic framework materials as chemical sensors", *Chem. Rev.*, Vol. 112, No. 2, pp. 1105-1125, 2012.
[37] J. Devkota, K.-J. Kim, P. R. Ohodnicki, J. T. Culp, D. W. Greve, and J. W. Lekse, "Zeolitic imidazolate framework-coated acoustic sensors for room temperature detection of carbon dioxide and methane", *Nanoscale*, Vol. 10, No. 17, pp. 8075-8087, 2018.
[38] J. Devkota, D. W. Greve, T. Hong, K.-J. Kim, and P. R. Ohodnicki, "An 860 MHz wireless surface acoustic wave sensor with a metal-organic framework sensing layer for CO_2 and CH_4", *IEEE Sens. J.*, Vol. 20, No. 17, pp. 9740-9747, 2020.
[39] D. Greve, J. Devkota, and P. Ohodnicki, "Wireless CO_2 SAW sensors with a nanoporous ZIF-8 sensing layer", *Proc. of 2018 IEEE International Ultrasonics Symposium (IUS)*, pp. 1-4, Kobe, Japan, 2018.
[40] F. A. Bahos, A. Sainz-Vidal, C. Sánchez-Pérez, J. M. Saniger, I. Gràcia, M. M. Saniger-Alba, and D. Matatagui, "ZIF nanocrystal-based Surface Acoustic Wave (SAW) electronic nose to detect diabetes in human breath", *Biosensors*, Vol. 9, No. 1, p. 4, 2018.
[41] S. I. Jung, I. R. Jang, C. Ryu, J. Park, A. M. Padhan, and H. J. Kim, "Graphene oxide decorated multi-frequency surface acoustic wave humidity sensor for hygienic applications", *Sci. Rep.*, Vol. 13, No. 1, p. 6838, 2023.
[42] F. Wang, J. Jian, X. Geng, G. Gou, W. Cui, J. Cui, Y. Qiao, J. Fu, Y. Yang, and T. L. Ren, "A miniaturized integrated SAW sensing system for relative humidity based on graphene oxide film", *IEEE Sens. J.*, Vol. 20, No. 17, pp. 9733-9739, 2020.
[43] Y. Zhang, Q. Tan, L. Zhang, W. Zhang, and J. Xiong, "A novel SAW temperature-humidity-pressure (THP) sensor based on $LiNbO_3$ for environment monitoring", *J. Phys. D Appl. Phys.*, Vol. 53, No. 37, p. 375401, 2020.
[44] X. Li, Q. Tan, L. Qin, L. Zhang, X. Liang, and X. Yan, "A high-sensitivity MoS_2/graphene oxide nanocomposite humidity sensor based on surface acoustic wave", *Sens. Actu-*

ators, A Phys., Vol. 341, p. 113573, 2022.
[45] S. Xu, R. Zhang, J. Cui, T. Liu, X. Sui, M. Han, F. Zheng, and X. Hu, "Surface acoustic wave DMMP gas sensor with a porous graphene/PVDF molecularly imprinted sensing membrane", *Micromachines*, Vol. 12, No. 5, p. 552, 2021.
[46] Q. Wu, X. Li, X. Wang, Y. Yuan, X. Bu, H. Wu, X. Li, C. Han, X. L. Wang, and W. Liu, "High-performance p-hexafluoroisopropanol phenyl functionalized multi-walled carbon nanotube film on surface acoustic wave device for organophosphorus vapor detection", *Nanotechnology*, Vol. 33, No. 37, p. 375501, 2022.
[47] S. Vizireanu, I. Constantinoiu, V. Satulu, S. D. Stoica, and C. Viespe, "High-sensitivity H_2 and CH_4 SAW sensors with carbon nanowalls and improvement in their performance after plasma treatment", *Chemosensors*, Vol. 11, No. 11, p. 566, 2023.
[48] M. I. A. Asri, M. N. Hasan, M. Nafea, Y. M. Yunos, and M. S. M. Ali, "Nanostructured Silicon-Based Surface Acoustic Wave Sensor for CO_2 Gas Detection", *IEEE Sens. J.*, Vol. 22, No. 24, pp. 23756-23764, 2022.
[49] F. Kus, C. Altinkok, E. Zayim, S. Erdemir, C. Tasaltin, and I. Gurol, "Surface acoustic wave (SAW) sensor for volatile organic compounds (VOCs) detection with calix [4] arene functionalized Gold nanorods (AuNRs) and silver nanocubes (AgNCs)", *Sens. Actuators B Chem.*, Vol. 330, p. 129402, 2021.
[50] M. Scarisoreanu, I. Constantinoiu, E. Goncearenco, I. P. Morjan, V. S. Teodorescu, and C. Viespe, "The Effect of Loading W&V: TiO_2 Nanoparticles with Noble Metals for CH_4 Detection", *Chemosensors*, Vol. 12, No. 8, p. 160, 2024.
[51] H. P. Kesuma, Q. Wang, A. A. Mohanan, and N. Ramakrishnan, "Mass loading characteristics of one-port SAW resonator with sensing film attached reflector electrodes", *IEEE Sens. Lett.*, Vol. 7, No. 12, pp. 1-4, 2023.
[52] J. Kim, H. Park, J. Kim, B.-I. Seo, and J.-H. Kim, "SAW chemical array device coated with polymeric sensing materials for the detection of nerve agents", *Sensors*, Vol. 20, No. 24, p. 7028, 2020.
[53] M. Tyona, "A theoritical study on spin coating technique", *Adv. Mater. Res.*, Vol. 2, No. 4, p. 195, 2013.
[54] A. Palla-Papavlu, S. I. Voicu, and M. Dinescu, "Sensitive materials and coating technologies for surface acoustic wave sensors", *Chemosensors*, Vol. 9, No. 5, p. 105, 2021.
[55] C. W. Extrand, "Spin coating of very thin polymer films", *Polym. Eng. Sci.*, Vol. 34, No. 5, pp. 390-394, 1994.
[56] Y. Yunus, N. A. Mahadzir, M. N. Mohamed Ansari, T. H. Tg Abd Aziz, A. Mohd Afdzaluddin, H. Anwar, M. Wang, and A. G. Ismail, "Review of the common deposition methods of thin-film pentacene, its derivatives, and their performance", *Polymers*, Vol. 14, No. 6, p. 1112, 2022.
[57] Y. Yan, J. Li, Q. Liu, and P. Zhou, "Evaporation Effect on Thickness Distribution for Spin-Coated Films on Rectangular and Circular Substrates", *Coatings*, Vol. 11, No. 11, p. 1322, 2021.
[58] X. Tang and X. Yan, "Dip-coating for fibrous materials: mechanism, methods and applications", *J. Sol-Gel Sci. Technol.*, Vol. 81, pp. 378-404, 2017.
[59] A. Mendoza-Galván, T. Tejeda-Galán, A. B. Domínguez-Gómez, R. A. Mauricio-Sánchez, K. Järrendahl, and H. Arwin, "Linear birefringent films of cellulose nanocrystals produced by dip-coating", *Nanomaterials*, Vol. 9, No. 1, p. 45, 2018.
[60] S. Alam, U. Mittal, and T. Islam, "The oxide film-coated surface acoustic wave resonators for the measurement of relative humidity", *IEEE Trans. Instrum. Meas.*, Vol. 70, pp. 1-9, 2021.
[61] A. K. S. Kumar, Y. Zhang, D. Li, and R. G. Compton, "A mini-review: How reliable is the drop casting technique?", *Electrochem. Commun.*, Vol. 121, p. 106867, 2020.
[62] C. Zuo, A. D. Scully, W. L. Tan, F. Zheng, K. P. Ghiggino, D. Vak, H. Weerasinghe, C. R. McNeill, D. Angmo, A. S. R. Chesman, and M. Gao, "Crystallisation control of drop-cast quasi-2D/3D perovskite layers for efficient solar cells", *Commun. Mater.*, Vol. 1, No. 1, p. 33, 2020.
[63] M. Eslamian and F. Soltani-Kordshuli, "Development of multiple-droplet drop-casting method for the fabrication of coatings and thin solid films", *J. Coat. Technol. Res.*, Vol. 15, No. 2, pp. 271-280, 2018.
[64] W. Li, J. Lin, X. Wang, J. Jiang, S. Guo, and G. Zheng, "Electrospray deposition of ZnO thin films and its application to gas sensors", *Micromachines*, Vol. 9, No. 2, p. 66, 2018.
[65] S. H. Park, L. Lei, D. D'Souza, R. Zipkin, E. T. DiMartini, M. Atzampou, E. O. Lallow, J. W. Shan, J. D. Zahn, D. I. Shreiber, H. Lin, J. N. Maslow, and J. P. Singer, "Efficient electrospray deposition of surfaces smaller than the spray plume", *Nat. Commun.*, Vol. 14, No. 1, p. 4896, 2023.
[66] F. Bender, L. Wachter, A. Voigt, and M. Rapp, "Deposition of high quality coatings on SAW sensors using electrospray", *Proc. of SENSORS, 2003 IEEE*, pp. 115-119, Toronto, Canada, 2003.
[67] S. Kavadiya and P. Biswas, "Electrospray deposition of biomolecules: Applications, challenges, and recommendations", *J. Aerosol Sci.*, Vol. 125, pp. 182-207, 2018.
[68] L. Chen, P. Degenaar, and D. D. Bradley, "Polymer transfer printing: application to layer coating, pattern definition, and diode dark current blocking", *Adv. Mater.*, Vol. 20, No. 9, pp. 1679-1683, 2008.
[69] M.-A. Yoon, C. Kim, J.-H. Kim, H.-J. Lee, and K.-S. Kim, "Surface properties of CVD-grown graphene transferred by wet and dry transfer processes", *Sensors*, Vol. 22, No. 10, p. 3944, 2022.
[70] X. Langston and K. E. Whitener, "Graphene transfer: a physical perspective", *Nanomaterials*, Vol. 11, No. 11, p. 2837, 2021.
[71] D. Zhang, Q. Zhang, X. Liang, X. Pang, and Y. Zhao, "Defects produced during wet transfer affect the electrical properties of graphene", *Micromachines*, Vol. 13, No. 2, p. 227, 2022.
[72] S. H. Kim, S. Jiang, and S.-S. Lee, "Direct CVD Growth of Transferable 3D Graphene for Sensitive and Flexible SERS Sensor", *Nanomaterials*, Vol. 13, No. 6, p. 1029, 2023.
[73] G. Wang, M. Zhang, Y. Zhu, G. Ding, D. Jiang, Q. Guo, S. Liu, X. Xie, P. K. Chu, Z. Di, and X. Wang, "Direct growth of graphene film on germanium substrate", *Sci. Rep.*, Vol. 3, No. 1, p. 2465, 2013.

[74] W. A. Groves, A. B. Grey, and P. T. O'shaughnessy, "Surface acoustic wave (SAW) microsensor array for measuring VOCs in drinking water", *J. Environ. Monit.*, Vol. 8, No. 9, pp. 932-941, 2006.

[75] M. S. Kamal, S. A. Razzak, and M. M. Hossain, "Catalytic oxidation of volatile organic compounds (VOCs)–A review", *Atmos. Environ.*, Vol. 140, pp. 117-134, 2016.

[76] X. Li, L. Zhang, Z. Yang, P. Wang, Y. Yan, and J. Ran, "Adsorption materials for volatile organic compounds (VOCs) and the key factors for VOCs adsorption process: A review", *Sep. Purif. Technol.*, Vol. 235, p. 116213, 2020.

[77] V. Soni, P. Singh, V. Shree, and V. Goel, "Effects of VOCs on human health", *in Air pollution and control*, N. Sharma, A. K. Agarwal, P. Eastwood, T. Gupta, and A. P. Singh, Eds. Springer, Singapore, pp. 119-142, 2018.

[78] A. Kansal, "Sources and reactivity of NMHCs and VOCs in the atmosphere: A review", *J. Hazard. Mater.*, Vol. 166, No. 1, pp. 17-26, 2009.

[79] M. Šetka, F. A. Bahos, O. Chmela, D. Matatagui, I. Gràcia, J. Drbohlavová, and S. Vallejos, "Cadmium telluride/polypyrrole nanocomposite based Love wave sensors highly sensitive to acetone at room temperature", *Sens. Actuators B Chem.*, Vol. 321, p. 128573, 2020.

[80] D. Matatagui, O. Kolokoltsev, J. M. Saniger, I. Gràcia, M. J. Fernández, J. L. Fontecha, and M. C. Horrillo, "Acoustic sensors based on amino-functionalized nanoparticles to detect volatile organic solvents", *Sensors*, Vol. 17, No. 11, p. 2624, 2017.

[81] C. Viespe and D. Miu, "Characteristics of surface acoustic wave sensors with nanoparticles embedded in polymer sensitive layers for VOC detection", *Sensors*, Vol. 18, No. 7, p. 2401, 2018.

[82] M. Šetka, F. A. Bahos, D. Matatagui, I. Gràcia, E. Figueras, J. Drbohlavová, and S. Vallejos, "Love wave sensors with silver modified polypyrrole nanoparticles for VOCs monitoring", *Sensors*, Vol. 20, No. 5, p. 1432, 2020.

[83] G. Kannan, A. Nimal, U. Mittal, R. Yadava, and J. Kapoor, "Adsorption studies of carbowax coated surface acoustic wave (SAW) sensor for 2, 4-dinitro toluene (DNT) vapour detection", *Sens. Actuators B Chem.*, Vol. 101, No. 3, pp. 328-334, 2004.

[84] A. L. Nikolaev, G. Ya. Karapetyan, D. G. Nesvetaev, N. V. Lyanguzov, V. G. Dneprovski, and E. M. Kaidashev, "Preparation and investigation of ZnO nanorods array based resistive and SAW CO gas sensors", *in Advanced Materials: Physics, Mechanics and Applications*, S. H. Chang, I. A. Parinov, and V. Y. Topolov, Eds. Springer, Cham, pp. 27-36, 2014.

[85] C. Lim, W. Wang, S. Yang, and K. Lee, "Development of SAW-based multi-gas sensor for simultaneous detection of CO_2 and NO_2", *Sens. Actuators B Chem.*, Vol. 154, No. 1, pp. 9-16, 2011.

[86] C. Wen, C. Zhu, Y. Ju, H. Xu, and Y. Qiu, "A novel NO_2 gas sensor using dual track SAW device", *Sens. Actuators A Phys.*, Vol. 159, No. 2, pp. 168-173, 2010.

[87] N. Dewan, S. Singh, K. Sreenivas, and V. Gupta, "Influence of temperature stability on the sensing properties of SAW NOx sensor", *Sens. Actuators B Chem.*, Vol. 124, No. 2, pp. 329-335, 2007.

[88] F. Klumpers, U. Götz, T. Kurtz, C. Herrmann, and T. M. Gronewold, "Conformational changes at protein–protein interaction followed online with an SAW biosensor", *Sens. Actuators B Chem.*, Vol. 203, pp. 904-908, 2014.

[89] Y. Yang, J. Jiang, T. Tuya, and C. Chaoluomeng, "Analysis of Bioproteins by Propagation Signal Based on SAW Device", *Proc. of 2019 4th International Conference on Communication and Information Systems (ICCIS)*, pp. 124-127, Wuhan, China, 2019.

[90] Y. Hur, J. Han, J. Seon, Y. E. Pak, and Y. Roh, "Development of an SH-SAW sensor for the detection of DNA hybridization", *Sens. Actuators A Phys.*, Vol. 120, No. 2, pp. 462-467, 2005.

[91] Z. Zhang, N. W. Emanetoglu, G. Saraf, Y. Chen, P. Wu, J. Zhong, Y. Lu, J. Chen, O. Mirochnitchenko, and M. Inouye, "DNA immobilization and SAW response in ZnO nanotips grown on LiNbO/sub$_3$/substrates", *IEEE Trans. Ultrason. Ferroelectr. Freq. Control*, Vol. 53, No. 4, pp. 786-792, 2006.

[92] A. Rydosz, "Sensors for enhanced detection of acetone as a potential tool for noninvasive diabetes monitoring", *Sensors*, Vol. 18, No. 7, p. 2298, 2018.

[93] D. Das, H. A. Chen, C. L. Weng, Y. C. Lee, S. M. Hsu, J. S. Kwon, and H. S. Chuang, "Rapid tear screening of diabetic retinopathy by a detachable surface acoustic wave enabled immunosensor", *Anal. Chim. Acta*, Vol. 1325, p. 343117, 2024.

[94] E. R. Gray, V. Turbé, V. E. Lawson, R. H. Page, Z. C. Cook, R. B. Ferns, E. Nastouli, D. Pillay, H. Yatsuda, D. Athey, and R. A. McKendry, "Ultra-rapid, sensitive and specific digital diagnosis of HIV with a dual-channel SAW biosensor in a pilot clinical study", *Npj Digital Med.*, Vol. 1, No. 1, p. 35, 2018.

[95] C.-Y. Lee and G.-B. Lee, "Humidity sensors: a review", *Sens. Lett.*, Vol. 3, No. 1-2, pp. 1-15, 2005.

[96] S. Sikarwar and B. Yadav, "Opto-electronic humidity sensor: A review", *Sens. Actuators A Phys.*, Vol. 233, pp. 54-70, 2015.

[97] T.-T. Wu, Y.-Y. Chen, and T.-H. Chou, "A high sensitivity nanomaterial based SAW humidity sensor", *J. Phys. D Appl. Phys.*, Vol. 41, No. 8, p. 085101, 2008.

[98] W. Jakubik, J. Wrotniak, C. Caliendo, M. Benetti, D. Cannata, A. Notargiacomo, A. Stolarczyk, and A. Kaźmierczak-Bałata "SAW Humidity Sensing with rr-P_3HT Polymer Films", *Sensors*, Vol. 24, No. 11, p. 3651, 2024.

[99] F. Sayar Irani and B. Tunaboylu, "SAW humidity sensor sensitivity enhancement via electrospraying of silver nanowires", *Sensors*, Vol. 16, No. 12, p. 2024, 2016.

[100] H. Yang, B. Shen, X. Liu, C. Jin, and T. Zhou, "A study on the gas/humidity sensitivity of the high-frequency SAW CO gas sensor based on noble-metal-modified metal oxide film", *Sensors*, Vol. 23, No. 5, p. 2487, 2023.

[101] X. Le, X. Wang, J. Pang, Y. Liu, B. Fang, Z. Xu, C. Gao, Y. Xu, and J. Xie, "A high performance humidity sensor based on surface acoustic wave and graphene oxide on AlN/Si layered structure", *Sens. Actuators B Chem.*, Vol. 255, pp. 2454-2461, 2018.